Sampling Requirements for Dynamic Cardiac PET Studies Using Image-Derived Input Functions

Raymond R. Raylman, John M. Caraher and Gary D. Hutchins

Department of Internal Medicine, Division of Nuclear Medicine, University of Michigan Medical Center, Ann Arbor, Michigan

The utilization of image-derived input functions is becoming common in quantitative PET studies of the heart. Consequently, imaging protocols must be designed to sample both blood and tissue concentrations adequately. Most clinical imaging protocols consist of a series of short initial scans to measure the rapid change in blood and tissue tracer concentration levels, followed by scans of gradually increasing length. The number of initial short scans must be matched to the shape of the input function. In this paper, noise-free simulation studies were performed to evaluate the effect of temporal sampling on estimates of the parameters of a two-compartment kinetic model. In addition, the consequences of varying tracer infusion length and timing were studied. The kinetic model parameters' bias decreased when infusion times were lengthened or sampling rates increased. Our results indicated that tracer infusions of 30 sec were best suited for these studies. Two currently employed clinical imaging protocols were then optimized for use with this infusion scheme. Ten initial scans with durations of 10 sec, or twenty of 5 sec length produced unbiased estimates of kinetic model parameters that describe myocardial physiology. Noisy simulations with the equivalent of one million events confirmed these results.

J Nucl Med 1993; 34:440–447

Investigation of cardiac physiology with positron emission tomography (PET) using complex acquisition protocols and quantitative data analysis is becoming more prevalent. Application of these methods for the evaluation of myocardial perfusion (*1–5*), metabolism (*6–8*) and neurophysiology (*9–13*) is currently being performed in a growing number of institutions. Many important factors such as tomograph count rate capabilities, scatter, attenuation and the influence of poor image resolution (tomograph and cardiac motion) have been investigated for cardiac PET (*14–17*). The estimation of the rate of physiological processes in cardiac PET involves the measurement of both myocardial tissue and arterial blood concentrations of a tracer as a function of time. In current state-of-the-art PET systems, the reconstructed image resolution is sufficient to enable the delineation of the radionuclide concentrations in the left atrium or ventricle of the heart (*18,19*). Therefore, image-based arterial blood curves can be substituted for direct arterial sampling from the patient, producing greatly simplified study protocols (*20*). When designing these quantitative cardiac PET protocols, temporal sampling schemes sufficient for the characterization of both the arterial blood and tissue time-activity curves should be developed.

Published investigations examining the optimization of kinetic 2-fluoro-2-deoxyglucose neurological PET studies have shown that study protocols using initial scans length of less than 30 sec duration produce very small errors in the estimation of kinetic rate constants (*21,22*). In each of these reports, input functions obtained from direct arterial sampling were used in the analysis. Since the radionuclide concentration in blood changes much more rapidly than the tissue concentration during the infusion stage, more demanding sampling requirements must be implemented to minimize errors in image-based input functions for quantitative cardiac PET studies. Herrero et al. (*23*) studied the effects of frame length, total scan duration and temporal shifting of the input function relative to the tissue curve on parameter estimation. These results demonstrated that these phenomena can cause significant bias.

In this work, we investigated the image sampling requirements for dynamic PET studies of the heart as a function of the input function shape using simulated data. Scanning protocols which reduced the bias and variance of kinetic model parameters were determined. The results of this study provide optimized imaging protocols for a variety of input function shapes.

MATERIALS AND METHODS

Noise-Free Sampled Input and Tissue Curve Simulation

Simulated noise-free data used in this study were produced utilizing a two-compartment model represented by:

Received May 15, 1992; revision accepted Nov. 4, 1992.

For correspondence or reprints contact: Raymond R. Raylman, PhD, University of Michigan Medical Center, 3480 Kresge III, Box 0552, Ann Arbor, MI 48109-0552.

TABLE 1
Clinical Imaging Protocols

	Protocol name	Imaging sequence
Coarse		
	A	2 × 10 sec, 3 × 20 sec, 2 × 60 sec, 2 × 150 sec, 4 × 300 sec
	B	3 × 10 sec, 3 × 20 sec, 2 × 60 sec, 2 × 150 sec, 4 × 300 sec
	C	4 × 10 sec, 3 × 20 sec, 2 × 60 sec, 2 × 150 sec, 4 × 300 sec
	D	5 × 10 sec, 3 × 20 sec, 2 × 60 sec, 2 × 150 sec, 4 × 300 sec
	E	6 × 10 sec, 3 × 20 sec, 2 × 60 sec, 2 × 150 sec, 4 × 300 sec
	F	7 × 10 sec, 3 × 20 sec, 2 × 60 sec, 2 × 150 sec, 4 × 300 sec
	G	8 × 10 sec, 3 × 20 sec, 1 × 60 sec, 2 × 150 sec, 4 × 300 sec
	H	9 × 10 sec, 3 × 20 sec, 1 × 60 sec, 2 × 150 sec, 4 × 300 sec
	I	10 × 10 sec, 3 × 20 sec, 1 × 60 sec, 2 × 150 sec, 4 × 300 sec
Fine		
	J	4 × 5 sec, 3 × 20 sec, 2 × 60 sec, 2 × 150 sec, 4 × 300 sec
	K	6 × 5 sec, 3 × 20 sec, 2 × 60 sec, 2 × 150 sec, 4 × 300 sec
	L	8 × 5 sec, 3 × 20 sec, 2 × 60 sec, 2 × 150 sec, 4 × 300 sec
	M	10 × 5 sec, 3 × 20 sec, 2 × 60 sec, 2 × 150 sec, 4 × 300 sec
	N	12 × 5 sec, 3 × 20 sec, 2 × 60 sec, 2 × 150 sec, 4 × 300 sec
	O	14 × 5 sec, 3 × 20 sec, 2 × 60 sec, 2 × 150 sec, 4 × 300 sec
	P	16 × 5 sec, 3 × 20 sec, 2 × 60 sec, 1 × 150 sec, 4 × 300 sec
	Q	18 × 5 sec, 3 × 20 sec, 2 × 60 sec, 1 × 150 sec, 4 × 300 sec
	R	20 × 5 sec, 3 × 20 sec, 2 × 60 sec, 1 × 150 sec, 4 × 300 sec

$$C_{sim}(t) = K_1 e^{-k_2 t} \otimes C_a(t), \quad \text{Eq. 1}$$

where $C_{sim}(t)$ is the simulated radionuclide concentration in a region of the myocardium, $C_a(t)$ is the input function and $\otimes$ represents the convolution operation. K_1 and k_2 are the standard two-compartment tracer transport parameters. The process of obtaining input functions from blood-pool images was simulated using the following equations:

$$C_{sa}(t_m) = \frac{1}{(t_2 - t_1)} \int_{t_1}^{t_2} C_a(t)\, dt \quad \text{Eq. 2}$$

$$t_m = \frac{t_1 + t_2}{2}.$$

$C_{sa}(t_m)$ is the simulated radionuclide concentration in the blood at time t_m. The values of t_1 and t_2 are the start and stop times of each frame. The parameter t_m is the mid-time between t_1 and t_2. $C_a(t)$ is an input function measured continuously (at 1-sec intervals) from a $H_2^{15}O$ PET study performed in our laboratory (*24*). The input function was integrated over the time limits set by the protocol. The result was then divided by the frame duration to produce input function data values in units of cps. Different infusion times were simulated by convolving the original input function with variable width step functions equal to the desired infusion times. Examples of the input functions used are shown in Figure 1A.

Tissue concentration sampling was simulated by integrating the analytical expression for the tissue response curve (Equation 1) over the individual frame times. This procedure is similar to that used to calculate the input function and is described by Equation 3:

$$C_{sc}(t_m) = \frac{1}{(t_2 - t_1)} \left[(1 - BV) \int_{t_1}^{t_2} C_{sim}(t)\, dt + BV \int_{t_1}^{t_2} C_a(t)\, dt \right], \quad \text{Eq. 3}$$

where $C_{sc}(t_m)$ is the sampled tissue response curve determined at the scan midpoints (t_m). BV is a parameter which represents the fraction of the input function which contributes to the measured region of interest (ROI) activity, $C_{sc}(t)$ (*5*). It reflects the amount of blood spillover present in a region caused by finite scanner resolution, cardiac motion and vascularization. The symbols $C_{sim}(t)$, $C_a(t)$, t_1 and t_2 are the same as those in the previous equations. A blood volume of 0.5 was used. This value has been shown to produce a good tradeoff between bias and variance (*25*). In the simulation, all data represent radionuclide concentrations corrected for radioactive decay.

Sampling Protocols

A series of scanning protocols consisting of uniform length frames, ranging in duration from 2 to 20 sec, was used to examine the frequency components of tissue and blood curves and corresponding modulation transfer functions. Each of these sequences was 1,800 sec in total duration. The protocols used to determine realistic optimal sampling sequences for PET studies were divided into two categories: coarse and fine. The coarse protocols consisted of frames with five different lengths. The first set were 10 sec long and were varied in number to find an optimum. The rest of the sequence contained three 20-sec frames followed by either one or two 60-sec frames, two 150-sec frames and four 300-sec frames. The longest of the coarse protocols was 1,750 sec long, the shortest was 1700 sec in duration. The fine scanning sequences utilized initial frames of 5 sec. The remainder of the fine scanning protocols were identical to the coarse sequences. Specific sampling protocols are listed in Table 1. The greatest difference in total length between any two of the protocols listed in this table is 50 sec. Herrero et al. (*23*) have demonstrated that kinetic parameters calculated using scanning protocols lasting more than 90 sec are insensitive to such small differences in length.

Frequency Response and Modulation Transfer Functions

The effect of different sampling rates on input function measurements was determined by calculating the frequency spectra of these functions. A discrete Fourier transform algorithm (*26*) was applied to the uninterpolated input functions sampled from the left ventricular blood pool. These data were simulated using Equation 2. A spectrum was calculated for sampling periods of 2, 4 and 8 sec. Modulation transfer functions (MTFs) were produced by taking the ratio of these spectra with the frequency spectrum calculated from the same input function sampled at a period of 1 sec. The bolus input function was used in order to demonstrate the worst-case effect of undersampling.

Sampling Induced Bias in Kinetic Rate Constants

The amount of bias caused by insufficient sampling and timing delay was determined by fitting the simulated data with Equation 4 using an unweighted nonlinear, least squares algorithm (*27*).

$$C_{sc}(t_m) = (1 - BV) \int_{t_1}^{t_2} K_1 e^{-k_2 t} \otimes C_{isa}(t)\, dt + BV \int_{t_1}^{t_2} C_a(t). \quad \text{Eq. 4}$$

$C_{isa}(t)$ was obtained by linearly interpolating $C_{sa}(t_m)$ onto a 1-sec grid. The values determined by the fitting procedure for K_1, k_2 and BV were then compared to the values supplied to the data simulation algorithm to assess the amount of bias and variance introduced by the sampling process. The infusion time was varied in order to determine its effect on bias.

In addition, we studied the sensitivity of different sampling sequences to temporal shifts of the input function. Unlike Herrero et al. (*23*), we utilized scan protocols that contained nonuniform length frames. These protocols are more representative of those used clinically. Delays from 0 to 20 sec were studied at four different flow states: K_1 = 1 ml/g/min, k_2 = 1/min; K_1 = 1 ml/g/min, k_2 = 0.3/min; K_1 = 0.2 ml/g/min, k_2 = 0.022 /min; and K_1 = 3 ml/g/min, k_2 = 0.3/min.

Noise Simulation

The effect of statistical noise on the sampling requirements was studied using a series of simulations. The first step in this process was to create a simulated dynamic heart phantom which possessed desired blood and tissue kinetics (*25*). This phantom model mimics the motion of the myocardium during the cardiac cycle. The radionuclide concentration in the myocardium and the blood pool was calculated using Equation 1 and the input function. The resulting digital dynamic heart phantom was "scanned" with a PET scanner simulator (*28*).

An ROI analysis method developed by Huesman (*29*) was used to produce the data that was to be fit. A circular ROI was placed in the left ventricle and another was placed in the center of the myocardium at a position where the blood volume fraction was approximately 0.5. The left ventricular region was used to determine the simulated input function. The ROIs were forward projected and filtered with a ramp filter to produce ROI sinograms. These sinograms were then multiplied by the emission sinograms. The resulting data were integrated to produce mean values and standard deviations for each ROI. Each plane contained the equivalent of 1 million true counts summed over all frames. The noise level for the fine protocols measured as the percent error (standard deviation/mean) at peak counts was approximately 9%. As in the case of the noise-free simulations, it was assumed that the data had been corrected for radioactive decay.

Given the mean and variance for each time point in each ROI, it is possible to create many different realizations of the data. A Gaussian distribution with the mean and variance specified by the ROI analysis routines was sampled to produce the noisy data. Two hundred realizations were produced for each ROI. The data from each realization were fit (using uniform weighting) with Equation 4. From these results it was possible to estimate how the presence of statistical noise affected the bias and variance produced by inadequate temporal sampling.

RESULTS

Simulated Tissue and Blood Curves

Examples of early portions of the arterial blood and myocardial tissue curves utilized in this study are shown in Figure 1. Panel A shows the simulated arterial blood curves for a bolus injection of tracer in addition to infusions of 30, 60 and 90 sec. In panel B, the effects of sampling on the image-derived input function from a bolus injection is demonstrated. Panel C shows the sampled input function obtained using a 30-sec infusion. In panel D, the simulated tissue-response to a 30-sec infusion is presented for a kinetic model configuration of K_1 = 1.0 ml/g/min and k_2 = 1.0/min.

Frequency Response and Modulation Transfer Functions

The Fourier transforms of the input functions shown in Figure 1A are presented in Figure 2. Increasing the infusion time of tracer administration acts like a low-pass filter, attenuating the high frequency content of the data. Figure 3 shows the MTFs for the uniform 2-, 4- and 8-sec sampling protocols. The loss of high frequency information with increasing sampling duration is evident.

Sampling Induced Bias in Kinetic Rate Constants

In Figure 4, the percent bias in kinetic rate constants is plotted as a function of uniform sampling period for the bolus and slow infusion input functions. This figure clearly demonstrates the significant levels of bias which result when the sampling protocol is not optimally matched to the blood and myocardial curve shapes.

The temporal relationship between the initiation of a sampling protocol and the arrival of the tracer in the heart also has a significant effect on the bias of kinetic rate constant estimates. Figure 5 demonstrates the range in bias in K_1 which may be observed as a function of PET sampling protocols for a 30-sec infusion.

Noise Simulation

Six combinations of sampling protocols and infusion times were selected to study the bias and variance caused by noise in the data. The outcome of 200 realizations are shown in Figures 6 and 7. The error due to counting statistics changed when differing numbers of total equiv-

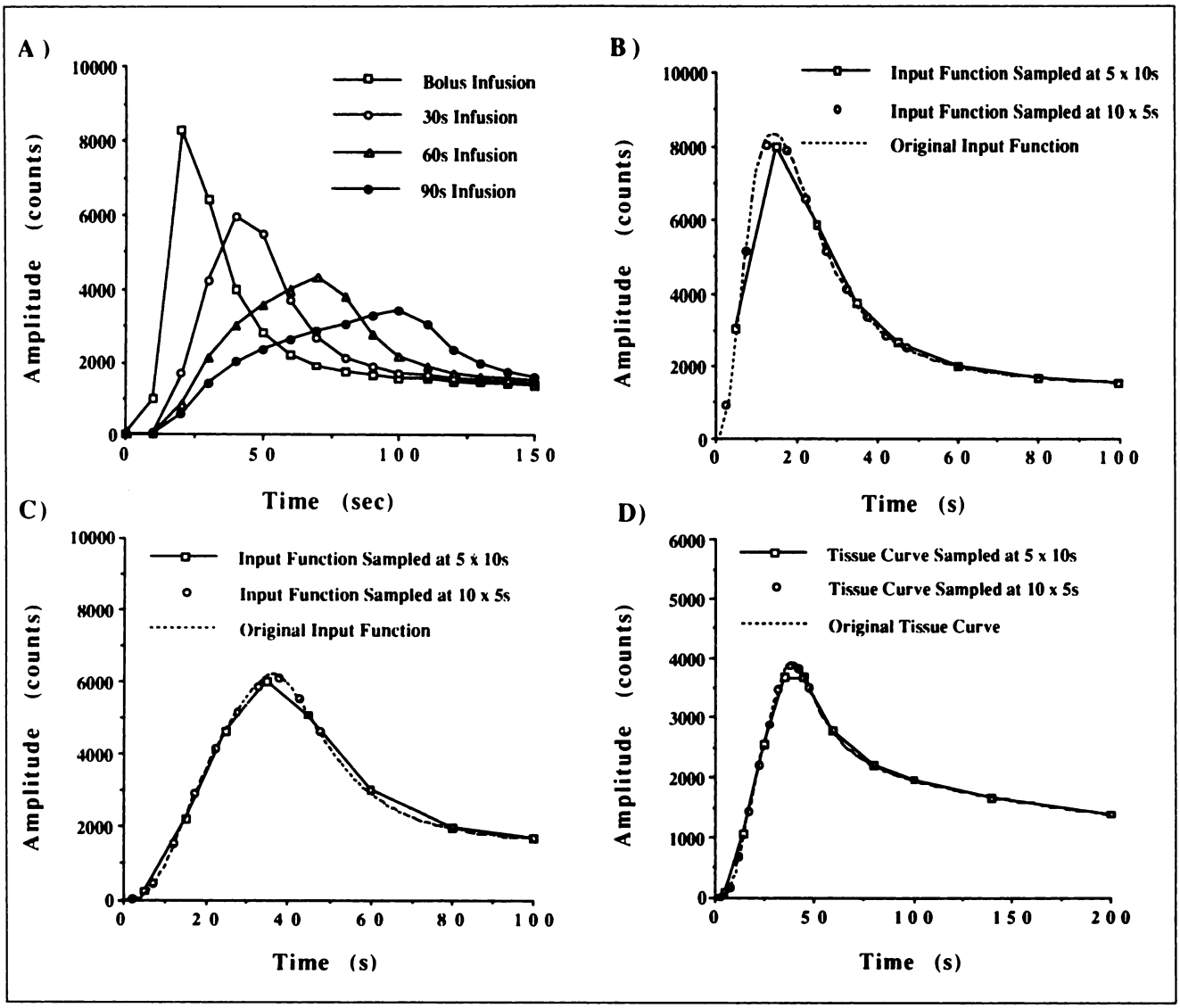

FIGURE 1. Input functions and tissue curves. (A) The four input functions used in the simulations. Each simulates a different infusion length. (B) Simulated sampled input functions using a bolus infusion. (C) A simulated sampled input function using a 30-sec infusion. (D) Simulated sampled tissue curve (K_1 = 1 ml/g/min, k_2 = 1 ml/g/min) from a 30-sec infusion.

alent counts were used. For example, decreasing the total number of counts to 500,000 increases the percent error from 9% to 15%. Likewise, the coefficient of variation (COV) increased from 30.5% to 53.44%. If the total number of counts is increased to 1.5 million, the percent error becomes 6.3% (at peak counts) and the COV is reduced to 27.4%. These results were calculated for the protocol using ten initial 5-sec frames.

DISCUSSION

Quantitative PET studies of cardiac physiology based upon tracer kinetic modeling principles require measurement of the temporal behavior of radiotracers in the arterial blood supply. While there are several systematic factors that can affect quantitative PET measurements (e.g., Compton scattering, motion and partial volume effects), insufficient temporal sampling of the data is a fundamental source of error. It therefore has a significant influence on the bias and variance of the parameter estimates calculated from the acquired data. In current state-of-the-art PET tomographs, image resolution is sufficient for the delineation of either the left ventricle or left atrium blood pool from myocardial tissue. In many of these studies, the positron-emitting tracer is administered as an intravenous bolus. This form of administration produces a rapidly changing concentration of the tracer in the arterial blood and myocardium during the initial minutes of the study. While bolus infusions are optimal from the standpoint of physiological parameter estimation, they impose important sampling requirements for PET. The balancing of the optimization of the image sampling protocols with the minimization of the total number of time

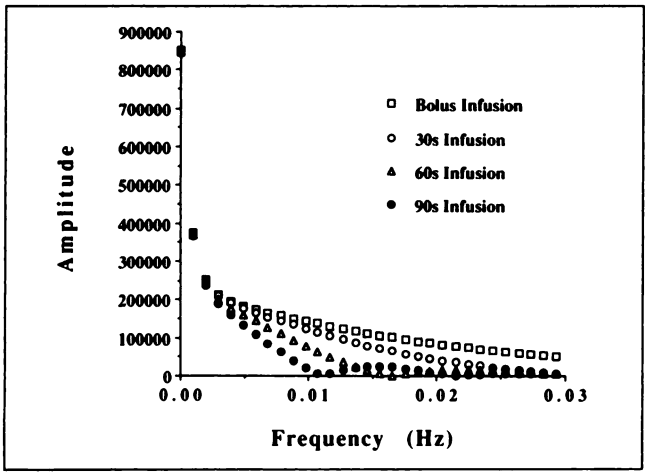

FIGURE 2. Input function Fourier spectra. The Fourier spectra of the four different input functions calculated from the curve in Figure 1A using a discrete Fourier transform algorithm.

points imaged in a routine study becomes an important concern.

Figure 2 shows the frequency spectrum of each of the input function shapes considered for this study. As expected, increasing the length of the tracer infusion attenuates the high frequency components of the input function. Since these functions are convolved with the mathematical model describing the underlying cardiac physiology, attenuating the frequency content of the input function is equivalent to attenuating myocardial tissue information used to estimate the physiological model parameters. In Figure 3, the MTFs for three uniform image sampling protocols are compared. It is evident from this figure that as the sampling duration is increased, the recovery of high frequencies in the input function become drastically impaired. The primary objective of

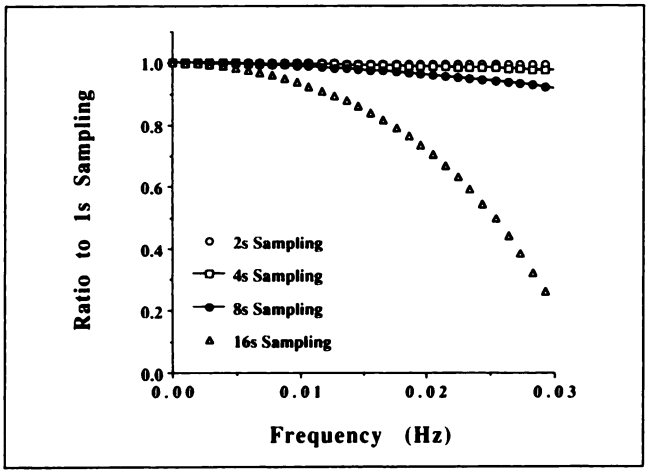

FIGURE 3. Modulation transfer functions. These functions were calculated from the bolus input function using four different scanning protocols. Each of the protocols utilized uniform length frames.

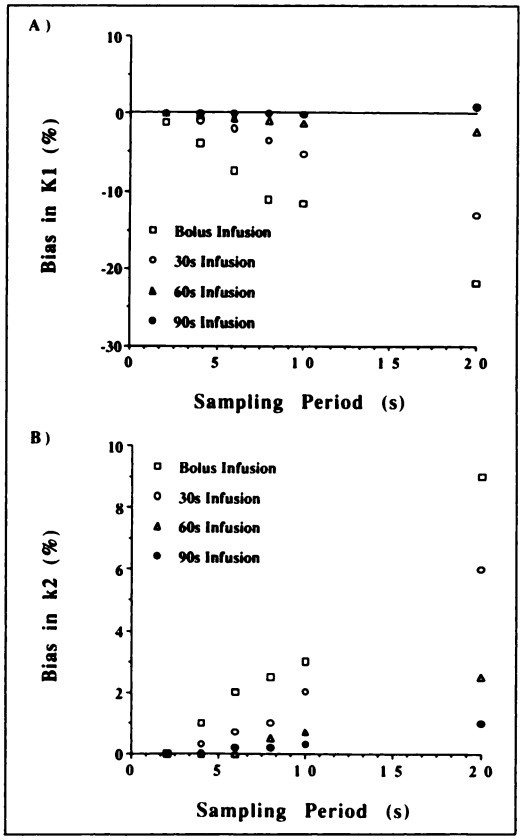

FIGURE 4. Noise-free uniform frame length results. (A) Bias in K_1 as a function of individual frame duration. (B) Bias in k_2 as a function of frame duration. For each plot, four different infusion times are shown.

the optimization studies therefore is to find the best balance between the loss of information due to input function shape and the loss due to the sampling protocol. In Figure 4, the combined effects of input function shape and sampling frequency on the estimates of parameters for a two-compartment model are demonstrated. These results represent noise-free simulations of both the myocardial and blood time-activity curves. Under these conditions, it is clear that the major factor which produces bias in kinetic rate constants is the relationship between sampling frequency and input function shape. The input function's shape does not significantly bias the rate constant estimates if the sampling is sufficient. This is demonstrated by the 60- and 90-sec infusion data. It should be noted that the bias in K_1 is much greater than that in k_2. This is to be expected, since the estimation of K_1 is much more dependent upon the sampling of the input function and the initial rise of the myocardial curve than is k_2. Therefore, K_1 bias caused by undersampling is especially sensitive to blood volume fractions and flow rates. Since the major effect is on K_1, the sampling recommendations we propose are applicable for use with any tracer kinetic compartmental model that has a single transport process between capillary blood and tissue. When statistical noise

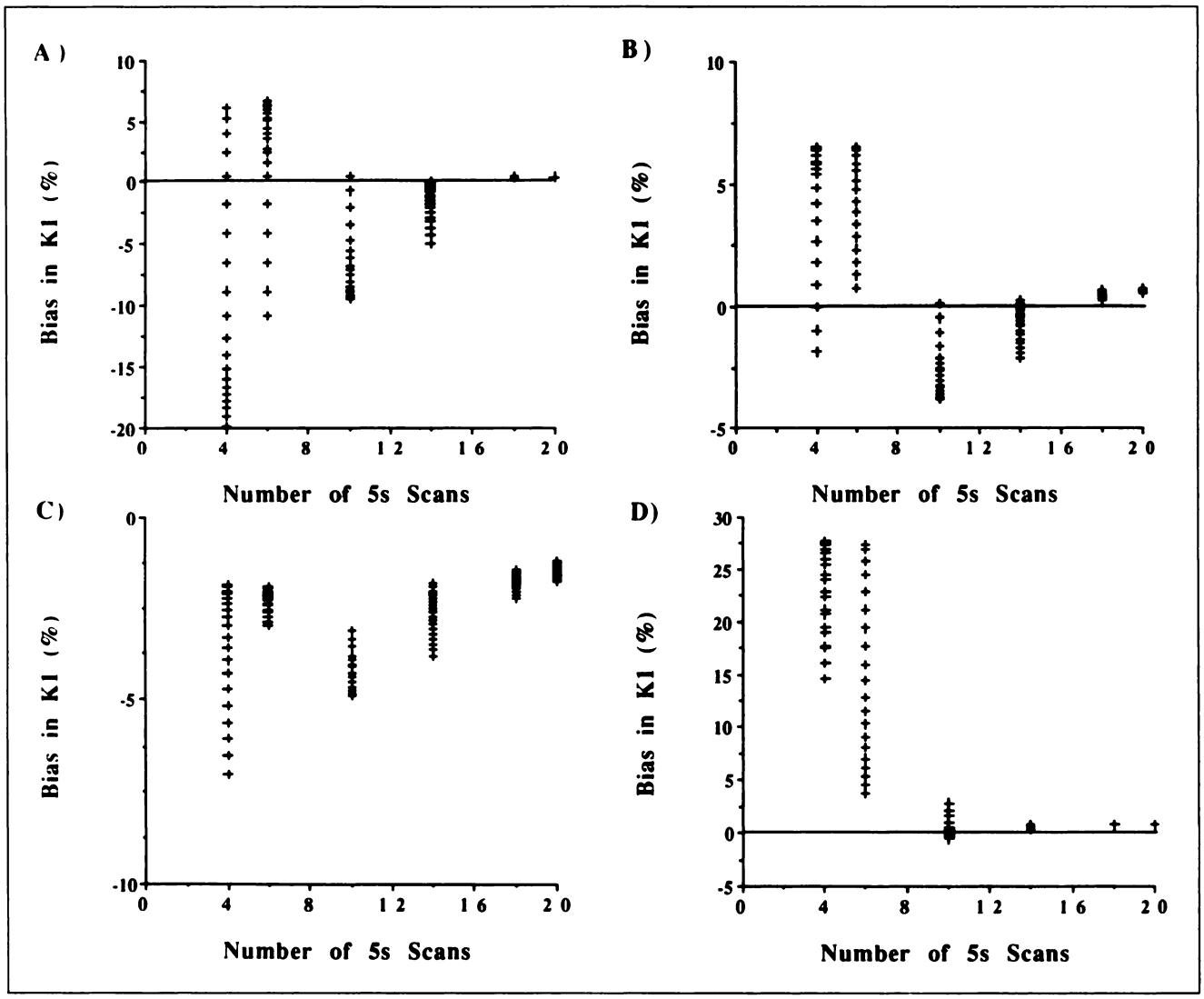

FIGURE 5. Bias in K_1 noise-free data using a fine protocol, 30-sec infusion. These plots show the percent bias in K_1 as a function of the number of initial 5-sec scans. Each plot presents the data for a different flow state: (A) K_1 = 1 ml/g/min, k_2 = 1/min, (B) K_1 = 1 ml/g/min, k_2 = 0.33/min, (C) K_1 = 0.2 ml/g/min, k_2 = 0.022/min and (D) K_1 = 3 ml/g/min, k_2 = 0.33/min. For each number of initial scans, the biases caused by infusion delays ranging from 0 to 20 seconds are shown. As the number of initial 5-sec scans is increased, the sampling bias is eliminated and 20 bias values are overlaid at the same point on the plot.

consistent with experimental PET studies is added, the variance in parameter estimates increases with increasing tracer infusion times (Figs. 6 and 7). The variance increase is the result of filtering produced by the infusion length.

When designing cardiac PET study protocols with a minimum number of images, an important consideration is the stability of the parameter estimates as a function of temporal alignment between tracer injection and the sampling protocol. When the scanning protocol chosen does not the meet the required sampling requirements, the bias in the parameters estimated from the resulting data shows high sensitivity to tracer arrival times. As the sampling protocols become more closely matched with the sampling requirements of the blood curve, the bias in the kinetic model parameters becomes independent of tracer arrival (Fig. 5). This plot also demonstrates that the relative kinetics of the myocardium can affect the bias. Since the input function is sharper than the tissue-response curves, it requires much higher sampling rates. Therefore, if the imaging protocol is matched to the input function, it will be *de facto* matched to the tissue curve. This is true even if blood-pool spillover into the myocardium is high.

A comparison of Figure 7 to Figure 5 demonstrates that the bias in K_1 is increased by the presence of statistical noise. This behavior is most likely due to the strong correlation between the input function and the tissue-response curve. The correlated error is not accounted for in the fitting process and therefore contributes to the bias.

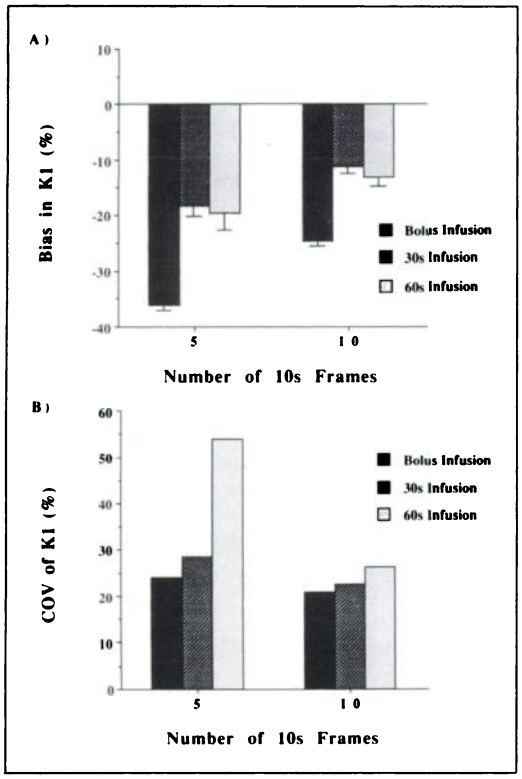

FIGURE 6. Noisy data results (coarse protocol). (A) Bias in K_1 calculated from 200 realizations. (B) COV calculated for K_1. The flow parameters were set at K_1 = 1 ml/g/min and k_2 = 1/min.

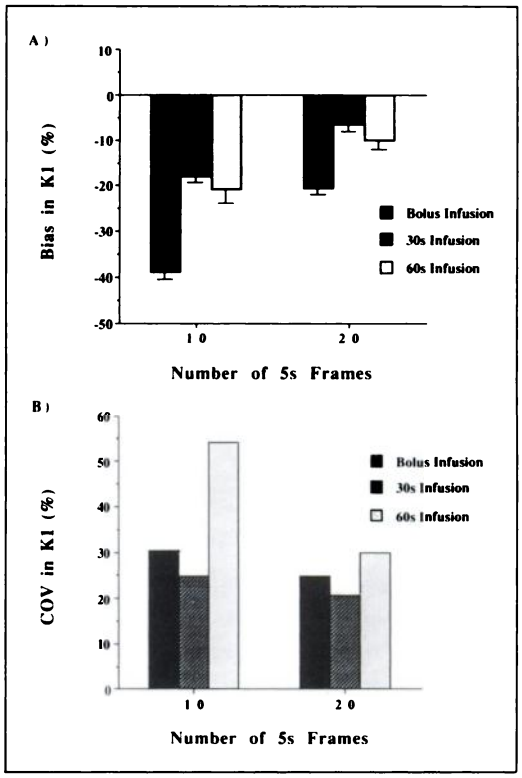

FIGURE 7. Noisy data results (fine protocol). (A) Bias in K_1 calculated from 200 realizations. (B) COV calculated for K_1. The flow parameters were set as K_1 = 1 ml/g/min and k_2 = 1/min.

Huesman and Mazoyer (*30*) have demonstrated that this condition introduces significant bias in K_1.

Clearly, it is important to carefully balance the choice of tracer infusion length and imaging protocol. The infusion duration should be short enough to minimize noise-induced variance, yet long enough to enable clinically useable scanning protocols to achieve sufficient temporal sampling of the input function. It must also sample the input function sufficiently to reduce sensitivity to temporal misalignment between the input function and tissue curve. Our investigation demonstrated that a 30-sec infusion most closely met these criteria. We limited the study to scanners whose shortest achievable frame length was 5 sec. If a scanner capable of shorter frames is available then the use of a shorter infusion time could be considered. Once the infusion length has been selected, the imaging protocol must be chosen. The major design parameters are the number and duration of the initial frames. The simulations were confined to protocols with 5- and 10-sec initial frames. The noise-free results showed that there must be at least ten 10-sec frames or twenty 5-sec frames to obtain stable and small biases in K_1 and k_2. The results from the noisy data confirmed that reductions in bias are obtained by following these guidelines. We have found that the COV is strongly dependent upon the number of counts contained in the study. A reduction in the number of total counts, and therefore the counts per frame, increased bias and variance. Also, reducing the length of the initial frames reduced bias, but increased variance. Thus, it is highly desirable to increase the number of counts per frame while decreasing their length. Our recommendations were made assuming the fitting algorithm applied a linear interpolation procedure to the tissue curves. It is likely that other interpolation methods (such as a spline fit) will produce slightly different input function curve shapes. This is due to the different responses these algorithms can have to undersampled data. Therefore, care should be exercised when implementing our suggested protocols.

CONCLUSION

In this work, the accuracy and precision of kinetic model parameters estimated from cardiac PET studies utilizing image-derived input functions were investigated as a function of input function shape and image sampling rate. From the results of this study, it is clear that care must be taken to match the input function with the imaging protocol to achieve minimum bias and variance in kinetic parameter estimates.

ACKNOWLEDGMENTS

Supported in part by a training grant from the National Cancer Institute, Washington DC and the Department of Energy, Washington, DC (DOE DE FG02-87ER).

REFERENCES

1. Wisenberg G, Schelbert HR, Hoffman EJ, et al. In vivo quantitation of regional myocardial blood flow by positron-emission computed tomography. *Circulation* 1981;63:1248–1258.
2. Bergmann SR, Fox KA, Rand AL, et al. Quantification of regional myocardial blood flow in vivo with $H_2^{15}O$. *Circulation* 1984;70:724–733.
3. Huang S-C, Schwaiger M, Carson RE, et al. Quantitative measurement of myocardial blood flow with oxygen-15-water and positron computed tomography: an assessment of potential problems. *J Nucl Med* 1985;26:615–625.
4. Krivokapich J, Smith GT, Huang S-C, et al. Nitrogen-13-ammonia myocardial imaging at rest and with exercise in normal volunteers: quantification of absolute myocardial perfusion with dynamic positron emission tomography. *Circulation* 1989;80:1328–1337.
5. Hutchins GD, Schwaiger M, Rosenspire KC, Krivokapich J, Schelbert H, Kuhl DE. Noninvasive quantification of regional blood flow in the human heart using N-13 ammonia and dynamic PET imaging. *J Am Coll Cardiol* 1990;15:1032–1042.
6. Schelbert HR. Assessment of myocardial metabolism by PET—a sophisticated dream or clinical reality? *Eur J Nucl Med* 1986;12:(suppl):S70–S75.
7. Kotzerke J, Hicks RJ, Wolfe E, et al. Three-dimensional assessment of myocardial oxidative metabolism: a new approach for regional determination of PET-derived carbon-11-acetate kinetics. *J Nucl Med* 1990;31:1876–1883.
8. Gould KL, Yoshida K, Hess MJ, Haynie M, Mullani N, Smalling RW. Myocardial metabolism of fluorodeoxyglucose compared to cell membrane integrity for the potassium analogue rubidium-82 for assessing infarct size in man by PET. *J Nucl Med* 1990;32:1–9.
9. Syrota A. In vivo study of receptors for nueromediator with PET. *Int J Rad Appl Instrum [B]* 1986;13:127–134.
10. Delforge J, Syrota A, Lancon JP, et al. Cardiac beta-adrenergic receptor density measured in vivo using PET, CGP12177, and a new graphical method. *J Nucl Med* 1991;32:739–748.
11. Syrota A. PET measurements of postsynaptic muscarinic and beta-adrenergic receptors in the heart. In: DE Kuhl, *Frontiers in nuclear medicine: in vivo imaging of neurotransmitter functions in brain, heart, and tumors.* Washington, DC: American College of Nuclear Physicians; 1990:363–392.
12. Wieland DM, Rosenspire KC, Hutchins GD, et al. Neuronal mapping of the heart with 6-[^{18}F] fluorometaraminol. *J Med Chem* 1990;33:956–964.
13. Schwaiger M, Hutchins GD, Kalff V, et al. Evidence for catecholamine uptake and storage sites in the transplanted human heart by positron emission topography. *J Clin Invest* 1991;87:1681–1690.
14. McCord ME, Bacharach SL, Bonow RD, Cuocolo A, Dilsizian V. Attenuation correction effects in the myocardium due to misalignment between transmission and emission PET scans [Abstract]. *J Nucl Med* 1990;31:736.
15. Bacharach SL, Freedman N, McCord ME, Bonow RD, Dilsizian V, Cuocolo A. The effect of spatially dependent deadtime on cardiac PET imaging [Abstract]. *J Nucl Med* 1990;31:777.
16. Bacharach SL, Vopio-Pulkki L-M, Perrore-Filardi P, et al. Correction of cardiac PET/SPECT for resolution and wall motion effects by gated NMR imaging [Abstract]. *J Nucl Med* 1991;32:938.
17. Spinks TJ, Araujo LI, Rhodes CG, Hutton BF. Physical aspects of cardiac scanning with a block detector positron tomograph. *J Comput Assist Tomogr* 1991;15:893–904.
18. Henze E, Huang S-C, Ratib O. Measurements of regional tissue and blood-pool radiotracer concentrations from serial tomographic images of the heart. *J Nucl Med* 1983;24:987–996.
19. Phelps ME, Mazziotta JC, Schelbert HR, eds. *Positron emission tomography and autoradiography.* New York: Raven Press; 1986.
20. Weinberg IN, Huang S-C, Hoffman EJ, et al. Validation of PET acquired input functions for cardiac studies. *J Nucl Med* 1988;29:241–247.
21. Hawkins RA, Phelps ME, Huang S-C. Effects of temporal sampling, glucose metabolism rates, and disruptions of the blood-brain barrier on the FDG model with and without a vascular component: studies in human brain tumors with PET. *J Cereb Blood Flow Metab* 1986;6:170–183.
22. Mazoyer BM, Huesman RH, Budinger TF, Krittel BL. Dynamic PET data analysis. *J Comput Assist Tomogr* 1986;10:653–654.
23. Herrero P, Markham J, Bergmann S. Quantitation of myocardial blood flow with $H_2^{15}O$ and positron emission tomography: assessment and error analysis of a mathematical approach. *J Comput Assist Tomogr* 1989;13:862–873.
24. Hutchins GD, Hichwa RD, Koeppe RA. A continuous flow input function detector for $H_2^{15}O$ blood flow studies in positron emission tomography. *IEEE Trans Nucl Sci* 1986;NS-33:546–549.
25. Hutchins GD, Caraher JM, Raylman RR. A region of interest strategy for minimizing resolution distortions in quantitative myocardial PET studies. *J Nucl Med* 1992;33:1243–1250.
26. Uhrich M. *Fast Fourier transform.* Bedford, MA: Raytheon Co.; 1968.
27. Marquardt DW. An algorithm for least-squares estimation of non-linear parameters. *J Soc Ind Appl Math* 1963;11:431–441.
28. Hutchins GD. Physiologic signal detection in positron emission tomography. In: DE Kuhl, ed. *Frontiers in nuclear medicine: in vivo imaging of neurotransmitter functions in brain, heart and tumors.* Washington, DC: American College of Nuclear Physicians; 1990:141–155.
29. Huesman RH. A new fast algorithm for the evaluation of regions of interest and statistical uncertainty in computed tomograph. *Phys Med Biol* 1984;29:543–552.
30. Huesman RH, Mazoyer BM. Kinetic data analysis with a noisy input function. *Phys Med Biol* 1987;32:1569–1579.